Effect of Smoothing during Transmission Processing on Quantitative Cardiac PET Scans

Nanette M.T. Freedman, Stephen L. Bacharach, Richard E. Carson, Julie C. Price and Vasken Dilsizian
Department of Nuclear Medicine, National Institutes of Health, Bethesda, Maryland

The effects of attenuation in cardiac PET are large and are produced by varied and inhomogeneous attenuating media. Although a measured attenuation correction can potentially provide an exact correction for attenuation, it introduces noise into the attenuation-corrected emission scan. Transmission smoothing reduces this noise but can introduce errors of its own. This study investigates these errors in absolute and relative quantitation and estimates their magnitude in a clinical setting. **Methods:** Fluorodeoxyglucose cardiac PET scans of 24 subjects were processed using measured attenuation correction with different levels of transmission smoothing. Mean activity concentrations were determined in septal, anterior and lateral regions of the left ventricle at each level of transmission smoothing. A theoretical derivation of the effects of transmission smoothing is presented, so that the observed effects could be compared with theory-based predictions. **Results:** In addition to the reduction of noise, transmission smoothing produced two further effects: (a) a previously unreported reduction in noise-induced bias, which is beneficial and (b) introduction of errors due to bad estimates of attenuation correction factors resulting from smoothing over regions where attenuation changes. The first effect was observed over all regions of the left ventricle, whereas the second reduced counts primarily in the lateral wall. Twenty-millimeter smoothing reduced noise-induced bias by an average of 4% (compared with 6-mm smoothing). This same smoothing caused an additional 9% decrease in the lateral wall as a result of the adjacent lung–lateral wall boundary. **Conclusion:** Transmission smoothing reduces both noise and noise-induced bias, but near transitions between differently attenuating media (e.g., lung-myocardial borders) may produce errors in absolute and relative quantitation. The data presented here document the magnitudes of these effects, permitting one to ensure that artifactually introduced inhomogeneities are kept small.

Key Words: PET; transmission smoothing; cardiac studies

J Nucl Med 1996; 37:690–694

Accurate correction for attenuation is a difficult and important challenge in PET. In view of the complexity of the attenuating structures in the chest, measured attenuation correction has generally been the technique of choice in cardiac imaging. Introduction of the rotating rod and fanbeam device (*1*) has reduced transmission scan duration and errors due to randoms and scatter, thus greatly increasing the potential for accurate attenuation correction. Because of practical limitations of scan duration, transmission scans are still count-limited and therefore noisy, which contributes additional noise to the emission scan (*2–6*). This transmission noise can produce visually noisier emission images (*2–5*), occasional streaking artifacts (*3*) and greater statistical uncertainty in quantitative estimates of activity (*2–4*). Another previously unreported consequence of transmission scan noise is the introduction of a noise-induced positive bias in the emission image.

In view of these undesirable consequences of transmission noise, transmission smoothing is often used. Emission images processed with smoothed transmission data are visually more acceptable and have fewer artifacts and less statistical noise (*3,4*). In the present article, we show that the noise-induced positive bias is also reduced. It has been reported, however, (*4,5*) that in addition to its beneficial effects, transmission smoothing can cause errors in phantom studies. Meikle et al. (*5*) have presented visual evidence of similar errors in a patient, study, but no quantitative data were given. Nevertheless, it appeared that the errors were different in different regions of the myocardium, indicating that errors in relative as well as absolute quantitation may result. These errors presumably arise because transmission smoothing introduces a mismatch in resolution between the smoothed transmission sinogram and the emission sinogram. Such a mismatch is well known to cause errors in attenuation-corrected emission scans (*2,4*), particularly near boundaries between differently attenuating media. Because of adjacent lung, the apical and free wall regions of the myocardium would be most susceptible to such errors, whereas septal regions would be least affected. Hence, errors in relative as well as absolute quantitation can be introduced.

Thus, smoothing transmission data reduces one source of error and worsens another. Errors resulting from statistical noise in the transmission scan are reduced, whereas those caused by resolution mismatch are increased. Therefore, the present work sought to determine the relative magnitude of these opposing errors, and thus their impact on quantitation, in cardiac scans in a series of 24 human subjects. The reduction of noise by transmission smoothing is well known (*2*). In the present article, we investigate a more subtle effect of transmission scan noise—the positive bias in the emission image as well as the errors due to resolution mismatch. Both of these errors can affect quantitation.

We derive an equation that can be used to compute the effect of transmission smoothing on bias in the emission image. The resolution mismatch effect is highly dependent on patient anatomy. We estimated its magnitude from the 24 clinical studies. Together, the equation and the clinical studies allow us to determine the degree of transmission smoothing that might best be used in clinical practice.

MATERIALS AND METHODS

Theory

We studied two effects of transmission smoothing: (a) reduction in the noise-induced bias in measured activity concentration and (b) artifactual inhomogeneities produced by transmission smoothing over regions with differing attenuation.

The first of these two effects, the noise-generated bias, is described mathematically in the Appendix. Attenuation correction factors (ACFs) are given by the ratio of counts in the blank and transmission scans. From Appendix 1, it can be seen that the expected value E of the ACF for an element in the sinogram, without transmission smoothing, is given approximately by:

Received Jan. 18, 1995; revision accepted Oct. 8, 1995.
For correspondence or reprints contact: Stephen Bacharach, PhD, Department of Nuclear Medicine, Bldg. 10, Room 1C-401, National Institutes of Health, Bethesda, MD 20892.

$$E\{ACF\} \approx \left(\frac{B}{m}\right)\left[1 + \frac{1}{m}\right], \qquad \text{Eq. 1}$$

where B is the value of counts obtained in one projection bin from a blank scan, and m is the mean value of the counts in the same bin in the transmission scan (scaled for differences in scan duration). The 1/m term in Equation 1 produces the bias seen in transmission scans at low count levels (m small); this term decreases as m increases. With transmission smoothing, Equation 1 becomes (see Appendix):

$$E\{ACF\} \approx \left(\frac{B}{m}\right)\left[1 + \frac{G}{m}\right], \qquad \text{Eq. 2}$$

where $G = \sum g_i^2$; and g_i represents the coefficients of the smoothing filter. For Gaussian filters, $G \leq 1$, so Equation 2 describes the desired reduction in bias obtained with smoothing.

The Appendix shows that for a Gaussian filter and fine projection sampling (projection sampling size $\ll$ FWHM), G is inversely proportional to the FWHM of the filter and is given approximately by:

$$G \approx \sqrt{(2 \log 2/\pi)}/\text{FWHM}. \qquad \text{Eq. 3}$$

Thus, the greater the FWHM, the smaller the positive bias in the ACFs, and for this case, Equation 2 becomes:

$$E\{ACF\} \approx \left(\frac{B}{m}\right)[1 + \sqrt{(2 \log 2/\pi)}/(\text{FWHM} \cdot m)]. \qquad \text{Eq. 4}$$

The second effect of transmission smoothing—introduction of inhomogeneity due to transmission smoothing over structures with differing attenuations—cannot be described with a mathematical formula because it is dependent on the location and properties of the attenuating structures within the subject. For images of the heart, these effects would be expected to be greatest in the neighborhood of lung boundaries because that is where the greatest changes in attenuation occur.

Cardiac PET Scans

Fluorine-18-deoxyglucose (FDG) studies were performed in 24 subjects (12 volunteers with no known cardiac disease and 12 patients with coronary artery disease) using a whole-body 21-slice scanner (43.5-cm diameter usable field of view; 11.5-cm axial length; 5.1-mm slice separation; 12.5-mm axial resolution; 7-mm in-plane reconstructed resolution; 1.7-mm pixel size and transverse sampling; 1.5-degree angular sampling). Blank and transmission scans were obtained using a rotating ^{68}Ge rod source (2–4 mCi) and fanbeam circuitry to reject coincident events not collinear with the rod source.

The 24 scans comprised a consecutive series of recent cardiac studies. Studies that were unsuitable for technical reasons (e.g., mispositioning or abnormally low overall FDG uptake) were excluded. Scans were acquired 30 min after injection of 5 mCi FDG during an acquisition time of 30 min. Myocardial concentration of FDG in a central slice averaged 1278 nCi/cc (s.d. 417) for the 24 subjects. Injection of FDG was preceded by a 30-min blank scan and a 15-min transmission scan. Average counts per projection bin in the part of the transmission sinogram corresponding to the center of the patient's chest ranged from about 6 to 10, depending on patient size (counts in individual bins in this region typically ranged from 0 to 30).

To calculate the ACFs, the blank and transmission sinograms were first corrected for wobble and then normalized for variations in detector uniformity (randoms and scatter corrections were not considered necessary because of use of a rotating rod source and fanbeam rejection). When smoothing was utilized, the blank and transmission sinograms were both smoothed separately (as described later). The blank was then divided by the transmission sinogram to generate a sinogram of ACFs. The emission sinogram was compensated for attenuation loss by multiplying by these ACFs.

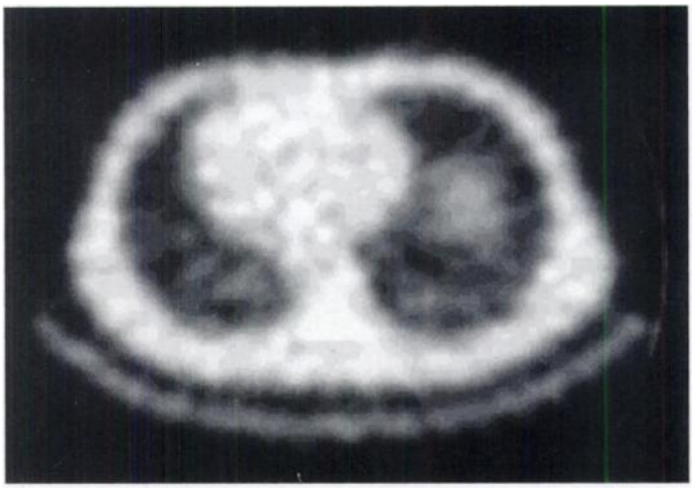

FIGURE 1. Attenuation image of entire body cross-section processed with 11-mm FWHM transmission smoothing.

In the present investigation, the blank and transmission sinograms for all 24 subjects were processed in five different ways: (a) with no smoothing, then (b)–(e) with smoothing using one-dimensional Gaussians, with a FWHM of 6, 11, 15 and 20 mm, respectively. The smoothing is one-dimensional, in the sense that it is only done along the spatial, not the angular, direction of the sinogram. In addition, 2- and 4-mm smoothing was performed in 3 of the 24 subjects.

The FDG emission sinogram for each subject was then attenuation-corrected with each set of ACFs and reconstructed to give five FDG images. The transaxial images of the heart were viewed, and for each subject three central contiguous slices intersecting the left ventricle (LV) were selected. Three regions of interest (ROIs) were drawn in each slice, corresponding to the septal, anterior and lateral walls of the LV, and the average measured activity concentration in each region over the three slices was computed. The activity concentrations obtained for all 24 subjects were examined to determine the degree to which they exhibited the effects of transmission smoothing previously described.

RESULTS

PET images of a typical transaxial slice through the myocardium are shown in Figures 1 (attenuation image) and 2 (FDG emission images). The visual effect of transmission smoothing is readily apparent from the FDG images shown with 2-, 6-, 11- and 20-mm FWHM transmission smoothing in Figure 2, a–d. Activity concentrations in ROIs drawn (Fig. 2e) over the lateral, anterior and septal regions of the LV were estimated from FDG images for all 24 subjects processed with all levels of transmission smoothing. Even in the normal myocardium, variations in FDG uptake around the myocardium may occur (*7,8*). To examine the effects of transmission smoothing on regional uptake, all data were (arbitrarily) normalized to the results at 6-mm smoothing. Ideally, one would have normalized all results to those obtained without smoothing. This normalization, however, was impractical because noise increased dramatically as the smoothing approached zero.

Figure 3 shows the changes in measured activity concentration in the lateral, anterior and septal walls of the myocardium, averaged over three central slices for all 24 subjects, as a result of transmission smoothing. Measured activity in all three

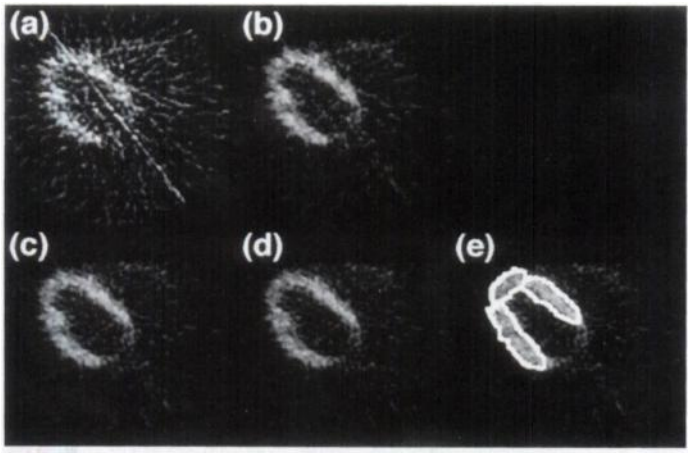

FIGURE 2. FDG emission images showing only the myocardium and area around it. Images (a)–(d) are processed with 2-, 6-, 11-, 20-mm FWHM transmission smoothing, respectively. Image (e) shows an example of ROIs drawn over the lateral, anterior and septal regions of the LV.

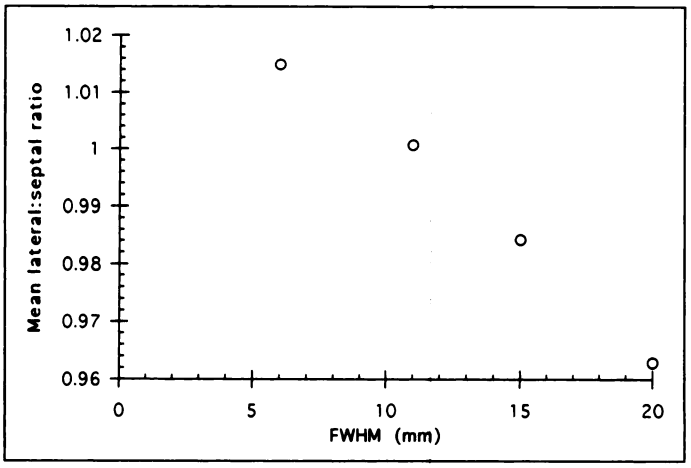

FIGURE 4. Variation with FWHM of transmission smoothing of ratio of mean activity concentrations in lateral/septal ROIs, averaged over 24 subjects.

regions decreased progressively with increased smoothing, but not at equal rates. For example, at 20-mm FWHM transmission smoothing, septal activity concentration was 0.96 of its value at 6-mm FWHM smoothing, and the corresponding fractions for the anterior and lateral regions were 0.95 and 0.91. Clearly, the changes relative to no smoothing would have been much greater had it been practical to measure them. These changes in measured activity with transmission smoothing were greatest in the lateral region, immediately adjacent to low-attenuation lung, and least in the septal region, adjacent to the right ventricle. Thus, increasing transmission smoothing produced a progressively decreasing lateral-to-septal wall ratio.

Lateral-to-septal wall ratios were calculated for all 24 subjects and were found to decrease with increasing transmission smoothing in each of the 24 subjects. Mean lateral-to-septal wall ratios are plotted in Figure 4. Here, normalization was not applied. Standard deviations are not shown because they mostly reflect the differences in absolute values of the lateral-to-septal wall ratio in this varied group of subjects and are not relevant to the effects of transmission smoothing. For all 24 subjects, the lateral-to-septal ratios were found to be artificially reduced from 1.015 at 6-mm smoothing to 1.001, 0.984 and 0.963 for 11-, 15- and 20-mm FWHM transmission smoothing, respectively. These decreases in lateral-to-septal ratio were statistically significant ($p < 0.001$, paired t-test) for all three levels of transmission smoothing.

The estimated activity concentrations were also examined to determine whether they followed the behavior predicted by Equation 4. Equation 4 describes the reduction in noise-generated bias with Gaussian transmission smoothing, predicting that mean counts will decrease linearly with the reciprocal of the smoothing FWHM. Estimates of the bias for Gaussian transmission smoothing with a FWHM of 2, 4, 6, 11, 15 and 20 mm were calculated from Equation 4 for a typical mean transmission scan count value (10 counts per element at the center of the sinogram). These estimates are shown in Table 1. In studies with lower counts, the bias may be much higher.

Figure 5 shows the observed decrease in measured activity concentration with increased smoothing (decreasing reciprocal of FWHM) for one of the three subjects whose data were transmission smoothed at 2-, 4-, 6-, 11-, 15- and 20-mm FWHM. The solid lines (straight-line fits to values at 6-mm FWHM smoothing and less) are shown to illustrate the deviation from the predicted linearity. When transmission smoothing was increased from 2 to 11 mm FWHM, the bias in this subject was reduced by approximately 5%, close to the typical value shown in Table 1. Thus, the estimated activity concentration in the septal ROI decreased approximately linearly with (1/FWHM). In contrast, the estimated activity concentration in the anterior ROI decreased nonlinearly at high FWHM (>11 mm), decreasing more than the linear decrease predicted by reduction in bias alone. Activity concentration in the lateral ROI showed even more dramatic deviation from the predicted linear decrease, with greater transmission smoothing. The behavior seen for this subject was typical of that for all 24 subjects.

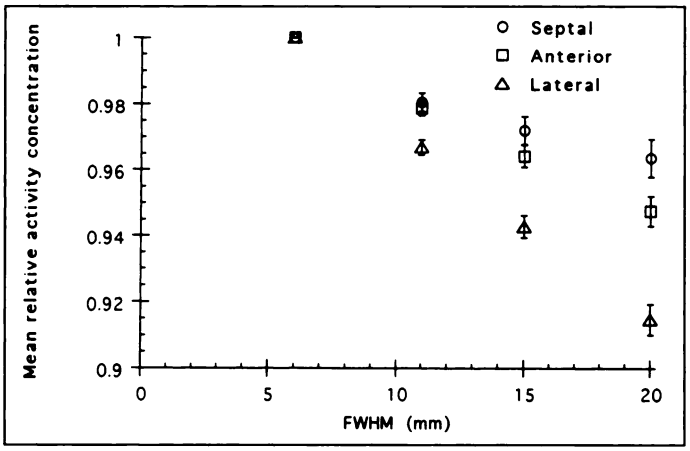

FIGURE 3. Mean activity concentrations in septal, anterior and lateral ROIs as a function of transmission smoothing. Activities were normalized to unity at 6-mm FWHM transmission smoothing and averaged over 24 subjects.

TABLE 1
Bias with Transmission Smoothing

FWHM of Gaussian smoothing filter (mm)	%Bias
2	5.6
4	2.8
6	1.9
11	1.0
15	0.8
20	0.6

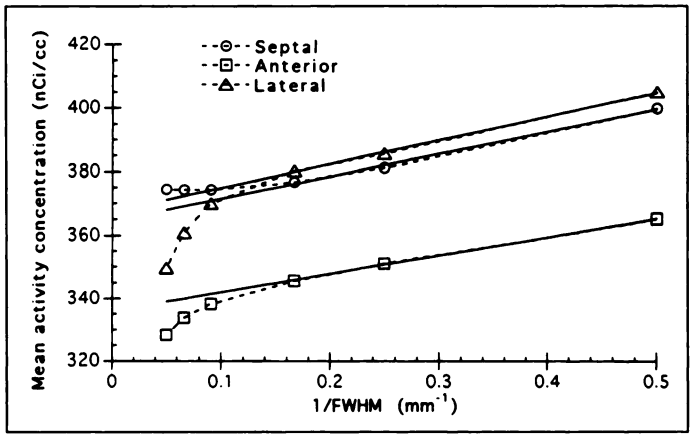

FIGURE 5. Variation in mean activity concentration in septal, anterior and lateral ROIs with inverse of FWHM for one subject. Dashed lines with symbols show the measured activity concentrations. Solid lines show the linear behavior extrapolated to greater transmission smoothing.

DISCUSSION

Measured myocardial activity was found to change with transmission smoothing. Both absolute and relative estimates of activity were affected. Three effects of transmission smoothing were observed: two were beneficial, the third detrimental. The two beneficial effects of transmission smoothing were the obvious reduction in noise in the attenuation-corrected emission scan and the observed decrease in bias at all regions around the heart. With no transmission smoothing, the activity values were positively biased because of noise in the transmission scan (as shown in the Appendix). Transmission smoothing lowered the absolute measured activity, reducing the bias. The detrimental effect caused by transmission smoothing was the introduction of artifactual myocardial inhomogeneity (manifested, e.g., by an erroneous decrease in the lateral/septal activity ratio).

The beneficial reduction in bias described earlier can be understood on an intuitive level. The ACF values go as the reciprocal of the transmission counts. A Poisson fluctuation in counts will cause a non-Poisson fluctuation in the reciprocal, resulting in the positive bias. Smoothing reduces the fluctuations in the denominator of the ACF and thereby reduces the bias.

The equations in the Appendix describe how smoothing reduces both bias and noise. They show that in a uniformly attenuating area, transmission smoothing reduces variance and improves estimates of the expected value of the ACFs. However, a real transmission scan in a human subject is far from uniform. Near the borders between two media with differing attenuation coefficients, the effects of transmission/emission resolution mismatch become important (*5*). As the width of the filter increases, transmission smoothing will smear lung attenuation values into myocardial regions, and vice versa, distorting the ACFs. This effect depends strongly on the detailed attenuation properties of the individual subjects and therefore cannot be analyzed mathematically or with phantoms. In smoothing patient data, it is therefore not obvious whether the intended beneficial or detrimental effects will dominate. The former beneficial reduction in noise and bias was shown (Fig. 5) to dominate in regions of approximately homogeneous attenuation (e.g., septal wall), whereas the detrimental effect of resolution mismatch dominated near boundaries between low and high attenuating media (e.g., lateral wall, near lung-myocardial borders).

How much transmission smoothing can be tolerated? Our results imply that for our system (or any other with similar resolution characteristics), use of transmission smoothing filters with greater than 11-mm FWHM can jeopardize accuracy of quantitation of relative as well as absolute activity concentrations around the myocardium. Figure 4 indicates that these effects are small, but they were seen consistently in all 24 subjects and may be clinically relevant in some circumstances.

Because the deleterious effects of transmission smoothing are dependent on scanner resolution, the level of smoothing at which they occur would vary for different scanners. The data presented here, however, could be modified to account for different scanner resolutions and different one-dimensional smoothing filters. Where two-dimensional sinogram smoothing is applied, the errors introduced are much more complex because smoothing along the angular direction of the sinogram introduces radial variations in resolution in the image.

In scanners with two acquisition modes, in which the low-resolution mode is conventionally used to reduce noise in transmission scans and the high-resolution mode is used for emission scans (*4*), the potentially deleterious effects of resolution mismatch will be present without explicit transmission smoothing. Segmentation of attenuation data can also result in resolution mismatch between transmission and emission data. Finally, transmission/emission resolution mismatch can also be caused by the use of isotopes with long positron ranges (e.g., ^{82}Rb). In this case, slightly greater transmission smoothing might be tolerated.

Unexplained heterogeneity of tracer uptake around the myocardium has been described in ^{13}N-ammonia and [^{18}F]FDG studies in healthy, normal volunteers (*7,8*), with the lateral and posterolateral segments having up to 10% to 20% lower counts than the anterior and septal regions. Figure 3 shows that for our system, transmission smoothing with a 20-mm FWHM Gaussian filter will on average result in a reduction of approximately 9% in counts in the lateral segment relative to counts in the septal region. Thus, transmission smoothing could have contributed to (but not entirely explained) this effect.

The results and discussion presented here pertain to cardiac studies only, that is, near regions lying immediately adjacent to a low-attenuation area such as the lungs. In other parts of the body, more transmission smoothing might well be tolerated without introducing significant error.

Despite the disadvantages associated with transmission smoothing, it is not clear that there are any better alternatives currently available. In cardiac imaging, the transmission sinogram is frequently very noisy, with very low counts in some projection bins. Noise reduction by extending scan duration is not practical. Because of the complexity and variety of attenuating structures in the chest, theoretical attenuation correction based on geometric models of structures cannot hope to adequately model the distribution of attenuation. Methods involving segmentation based on a real transmission scan (*5,9,10*) show some potentially encouraging results. Reconstruction-reprojection has been shown to perform less well than smoothing for low-count transmission scans (*6*). Future PET scanners may be capable of acquiring high-count transmission scans within a realistic scan time, reducing the need for transmission smoothing. The increasing complexity of scanning procedures (e.g., whole-body scans) will continue to demand ever-shorter transmission scan durations, thus extending the need for transmission smoothing. Thus, transmission smoothing continues to be widely applied, and a thorough understanding of its benefits as well as the errors that it may introduce remain important. The present work indicates that, provided that care is exercised in the choice of the smoothing filter, the resulting errors can be kept small.

CONCLUSION

The present report describes how transmission smoothing can affect quantitative estimates of activity in the myocardium. Increasing degrees of transmission smoothing reduce noise in the corrected emission image and improve estimates of absolute counts, but distort regional variations in measured myocardial activity. Although the changes we observed are statistically significant, they are small and may not be of clinical relevance in assessing pathologic cardiac scans. The changes may be important in evaluating the smaller inhomogeneities that have been reported in normal subjects. Because the magnitudes of the effects of transmission smoothing are machine- and isotope-dependent and certainly vary with choice of smoothing filter, their importance must be evaluated for each situation.

APPENDIX: BIAS IN ATTENUATION CORRECTION FACTORS

Noise in the transmission scan introduces bias and noise into the ACFs. These effects can be described mathematically. The ACF in a bin in the sinogram equals B/T, where B is the value of counts obtained from a blank scan (appropriately scaled), and T is the value of counts from the transmission scan. Because a high-count blank scan can be obtained with no difficulty, noise in the blank scan will be ignored here. T is a sample from a Poisson-distributed population with mean m and variance m. We wish to examine the effect of the noise distribution of T on the expected value of B/T. The Taylor series expansion for the function $f(T) = B/T$ about $T = m$ is given by:

$$f(T) = \frac{B}{m} - (T - m)\frac{B}{m^2} + (T - m)^2\frac{B}{m^3} + \text{Higher order terms.} \qquad \text{Eq. A1}$$

We can now write the expected value E of f(T) approximately as

$$E\{f(T)\} \approx \frac{B}{m} - E\{(T - m)\}\frac{B}{m^2} + E\{(T - m)^2\}\frac{B}{m^3}, \qquad \text{Eq. A2}$$

neglecting higher order terms. Because $E\{(T - m)\} = 0$, and $E\{(T - m)^2\}$ is by definition the variance of T, var (T), we now have

$$E\{f(T)\} = E\{ACF\} \approx \left(\frac{B}{m}\right)\left[1 + \frac{\text{var}(T)}{m^2}\right]. \qquad \text{Eq. A3}$$

For the Poisson distribution, $\text{var}(T) = m$; hence, Equation A3 can be rewritten as:

$$E\{ACF\} \approx \left(\frac{B}{m}\right)\left[1 + \frac{1}{m}\right]. \qquad \text{Eq. A4}$$

Thus, the expectation value of the ACF is not simply the blank B divided by the mean transmission counts m; it is larger than this by a factor of $[1 + (1/m)]$. Therefore, the noisier the transmission scan, the higher the values of the ACFs. For example, if a sinogram pixel has 10 transmission counts, its ACF will be overestimated by 10%, whereas for a pixel with 100 transmission counts, the overestimate is only 1%. This behavior occurs because the ACF is dependent on the *inverse* of the transmission counts.

This mathematical description can be extended to describe the effects of a count-preserving smoothing filter. In this case, after smoothing, the value in a transmission sinogram bin is given by

$$T = \sum g_i t_i, \qquad \text{Eq. A5}$$

where t_i represents the original unsmoothed transmission counts in the surrounding bins and g_i the coefficients of the smoothing filter. Note that because the smoothing filter is count preserving, $\sum g_i = 1$. Now, $m = E\{T\} = \sum g_i m_i$, where $m_i = E\{t_i\}$, and $\text{var}(T) = \sum g_i^2\,\text{var}(t_i) = \sum g_i^2 m_i$, assuming statistical independence of sinogram values. Substituting into Equation A3, we can now write the equation for the expected value of B/T (where T now represents the smoothed transmission counts), as follows:

$$E\{ACF\} \approx \left(\frac{B}{m}\right)\left[1 + \frac{\sum g_i^2 m_i}{m^2}\right]. \qquad \text{Eq. A6}$$

In small neighborhoods, where m_i is reasonably constant, this reduces to:

$$E\{ACF\} \approx \left(\frac{B}{m}\right)\left[1 + \frac{G}{m}\right], \qquad \text{Eq. A7}$$

where $G = \sum g_i^2$. For a filter function that is real and nonnegative in the spatial domain, $G \leq 1$, so that this form of smoothing will always result in lower bias in the ACFs than would be obtained in the absence of smoothing. The reduction in the ACF will depend on G for the smoothing filter used. The factors g_i in the continuous case are given by the normalized Gaussian as $g(x) = (2/f)\sqrt{(\log 2/\pi)}\exp(-4\log 2x^2/f^2)$, and $\sum g_i^2$ reduces to the integral $\int_{-\infty}^{\infty} g^2(x)\,dx$, which can be easily shown (*11*) to vary as $\sqrt{(2\log 2/\pi)}/f$. Therefore, the larger the smoothing FWHM, the smaller the G and the less the positive bias in the ACFs. With adequate sampling, this result also holds in the discrete case.

REFERENCES

1. Carroll LR, Kertz P, Orcut G. The orbiting rod source: improving performance in PET transmission correction scans. In: Esser PD, ed. *Emission computed tomography: current trends*. New York: Society of Nuclear Medicine; 1983:235–247.
2. Huang S-C, Hoffmann EJ, Phelps ME, Kuhl DE. Quantitation in positron emission computed tomography: II. Effects of inaccurate attenuation correction. *J Comput Assist Tomogr* 1979;3:804–814.
3. Dahlbom M, Hoffmann EJ. Problems in signal-to-noise ratio for attenuation correction in high resolution PET. *IEEE Trans Nucl Sci* 1987;34:288–293.
4. Palmer M, Rogers JG, Bergstrom M, Beddoes MP, Pate BD. Transmission profile filtering for positron emission tomography. *IEEE Trans Nucl Sci* 1986;33:478–481.
5. Meikle SR, Dahlbom M, Cherry S. Attenuation correction using count-limited transmission data in positron emission tomography. *J Nucl Med* 1993;34:143–150.
6. Ollinger JM. Reconstruction-reprojection processing of transmission scans and the variance of PET images. *IEEE Trans Nucl Sci* 1992;39:1122–1125.
7. Porenta G, Kuhle W, Czernin J, et al. Semiquantitative assessment of myocardial blood flow and viability using polar map displays of cardiac PET images. *J Nucl Med* 1992;33:1623–1631.
8. Gropler RJ, Siegel BA, Lee KJ, et al. Nonuniformity in myocardial accumulation of fluorine-18-fluorodeoxyglucose in normal fasted humans. *J Nucl Med* 1990;31:1749–1756.
9. Xu EZ, Mullani NA, Gould KL, Anderson WL. A segmented attenuation correction for PET. *J Nucl Med* 1991;18:161–165.
10. Price JC, Bacharach SL, Freedman N, Carson RE. Noise reduction in PET attenuation correction by maximum likelihood (ML) histogram sharpening of attenuation images [Abstract]. *J Nucl Med* 1993;34(suppl):27P.
11. William H Beyer, ed. *CRC handbook of mathematical sciences*, 5th ed. Boca Raton, FL: CRC Press; 1980:441.